

# Statistics of level spacing of geometric resonances in random binary composites

Y. Gu<sup>1,2</sup> and K. W. Yu<sup>2</sup>

<sup>1</sup>*Mesososcopic Physics Laboratory, Department of Physics,  
Peking University, Beijing 100871, China*

<sup>2</sup>*Department of Physics, The Chinese University of Hong Kong,  
Shatin, New Territories, Hong Kong, China*

Z. R. Yang

*Department of Physics, Beijing Normal University,  
Beijing 100875, China*

## Abstract

We study the statistics of level spacing of geometric resonances in the disordered binary networks. For a definite concentration  $p$  within the interval  $[0.2, 0.7]$ , numerical calculations indicate that the unfolded level spacing distribution  $P(t)$  and level number variance  $\Sigma^2(L)$  have the general features. It is also shown that the short-range fluctuation  $P(t)$  and long-range spectral correlation  $\Sigma^2(L)$  lie between the profiles of the Poisson ensemble and Gaussian orthogonal ensemble (GOE). At the percolation threshold  $p_c$ , crossover behavior of functions  $P(t)$  and  $\Sigma^2(L)$  is obtained, giving the finite size scaling of mean level spacing  $\delta$  and mean level number  $n$ , which obey the scaling laws,  $\delta = 1.032L^{-1.952}$  and  $n = 0.911L^{1.970}$ .

PACS number(s): 77.84.Lf, 42.65.-k, 02.50.-r

## I. INTRODUCTION

Random matrix theory (RMT) originated from dealing with the energy levels of complex many-body quantum systems has become an independent new statistics.<sup>1</sup> Different from the standard statistics in physics, RMT focuses its attention on the general properties of a number of stochastic ensembles with common symmetry. The correlation and fluctuation of eigenvalues and eigenfunctions in random Hamiltonian systems are the central issues in the applications of RMT. Apart from the nuclear and nuclei fields, it was also employed to study the critical statistics of disordered systems with various complex interaction.<sup>2–7</sup> Recently, resonant properties of composite materials have been studied extensively due to the large linear and nonlinear optical responses.<sup>8–12</sup> In a dielectric network, there exist a lot of geometric resonances randomly distributing in the resonant area.<sup>13–16</sup> For a specific sample, its resonance spectrum is very sensitive to the microstructure. While, for a large number of samples given a parameter, i.e., concentration  $p$ , the distribution of resonances is stable, which implies some general features of resonance spectrum. The aim of this paper is to study the level spacing statistics of geometric resonances.

In this work, a binary network is considered, where the impurity bonds with admittance  $\epsilon_1$  are employed to replace the bonds in an otherwise homogeneous network of identical admittance  $\epsilon_2$ . The admittance of each bond is generally complex and frequency-dependent. All the impurity bonds construct the clusters subspace. For a binary composite, the admittance ratio  $h(= \frac{\epsilon_1}{\epsilon_2})$  of two components has a branch cut on the negative axis when resonance happens.<sup>17</sup> Based on the Green's-function formalism (GFF), the eigenvalues( $s = \frac{1}{1-h}$  and  $s \in [0, 1]$ ) of Green's-matrix  $M$  are solved, the sequence of which forms the resonance spectrum.<sup>13,15</sup>  $M$  maps the geometric configuration of the clusters subspace. Its solutions summarize the geometric resonances of the network subject to the external sources and in the quasistatic limit. The element of  $M$  is defined as  $M_{\mathbf{x},\mathbf{y}} = \sum_{\mathbf{z} \in C(\mathbf{y})} (G_{\mathbf{x},\mathbf{y}} - G_{\mathbf{x},\mathbf{z}})$ , where  $\mathbf{z} \in C(\mathbf{y})$  means that the jointing points  $\mathbf{z}$  and  $\mathbf{y}$  belong to the impurity metallic cluster and are the nearest neighbors. More clearly,  $M_{\mathbf{x},\mathbf{y}}$  describes the interaction between  $\mathbf{x}$  and  $\mathbf{y}$  and is closely related to the “environment” or the nearest neighbors of  $\mathbf{y}$ . In a dilute network, there exists a large “environment” difference between two jointing points, hence the elements of  $M$  distribute more uncorrelatively rather than with some symmetry. However, for a percolating network, due to the self-similar structure,  $\mathbf{x}$  and  $\mathbf{y}$  have the similar “environment” and  $M_{\mathbf{x},\mathbf{y}}$  is approximately equal to  $M_{\mathbf{y},\mathbf{x}}$ . It is analogous to the Gaussian orthogonal ensemble (GOE), in which the elements of the Hamiltonian matrix must satisfy  $H_{m,n} = H_{n,m}$ . So, for a disordered composite, it is expected that the correlation and fluctuation of eigenvalues of  $M$  have the general features.

In the following, statistics of resonance level spacing in the disordered binary composites is studied intensively on the unfolded scale. For one sample, there are more than 700 levels numerically solved by its Green's-matrix  $M$ . In the unfolding procedure, we use a fit of the third order polynomial to the data. For an arbitrary  $p$ , 1000 samples, with totally more than 700,000 levels, are computed for the sake of the ensemble averaging. For a definite  $p$  within the interval  $[0.2, 0.7]$ , our numerical calculations indicate that the unfolded level spacing distribution  $P(t)$  and level number variance  $\Sigma^2(L)$  have the general features. It is also shown that the short-range fluctuation  $P(t)$  and long-range spectral correlation  $\Sigma^2(L)$  lie between the profiles of the Poisson ensemble and GOE.

This paper is organized as follows. In the next two sections, for various  $p$ , level spacing distributions  $P(t)$ 's and level number variances  $\Sigma^2(L)$ 's are calculated on the unfolded scale. Then, in Section IV, at  $p_c$ , crossover behavior of  $P(t)$  and  $\Sigma^2(L)$  is obtained, giving the finite size scaling of mean level spacing  $\delta$  and mean level number  $n$ . Finally, we summarize the main results in Section V.

## II. UNFOLDED LEVEL SPACING DISTRIBUTION

In order to remove the system-specific mean level density or normalize the resonance level spacing of different samples, unfolding procedure is necessary. For a sample, the cumulative spectral function  $C(s)$  of its resonance spectrum is defined as<sup>1</sup>

$$C(s) = \int_{-\infty}^s f(s') ds', \quad (1)$$

where  $f(s') = \sum_{n=1}^N \delta(s' - s_n)$  is the spectral function of levels. When  $N \rightarrow \infty$ ,  $f(s')$  should be smooth.  $C(s)$  is the staircase function and is used to count the number of levels. To satisfy that  $f(s')$  is smooth,  $s$  is rescaled by  $\xi$  as

$$C(s) = \xi + C_{fl}(s), \quad (2)$$

where  $\xi$  is the smooth part of  $C(s)$  and  $C_{fl}(s)$  is the fluctuating part of  $C(s)$ . Fig. 1 shows the small section of the measured spectrum. In the following, we use the third order polynomial to fit the data. However, when  $p = 0.1$  or  $0.2$ , the ninth or eleventh polynomial is not high enough to fit the curve because of the large fluctuation of level spacing. So at the dilute systems, numerical calculations are not accurate.

The level spacing distribution  $P(t)$  is the probability density for neighboring levels  $\xi_n$  and  $\xi_{n+1}$  having the spacing  $t$ . It is used to describe the short-range spectral fluctuations. On the unfolded scale, the function  $P(t)$  and its first moment are normalized to unity,  $\int_0^\infty P(t) dt = 1$  and  $\int_0^\infty t P(t) dt = 1$ . For the uncorrelated or Poisson ensemble  $P_p(t) = \exp(-t)$ , while for the GOE, or Wigner-Dyson ensemble,  $P_{WD}(t) = \frac{\pi}{2t} \exp(-\frac{\pi^2 t}{4})$ . Fig. 2 displays the level spacing distributions  $P(t)$ 's for various  $p$  within the interval  $[0.1, 0.7]$ . In this figure, the distributions  $P_p(t)$  and  $P_{WD}(t)$  are drawn by the dashed and solid lines respectively. The solid curves with the filled or opaque circles represent the critical distributions  $P_T(t)$  at the percolation threshold  $p_c$ . The inset of Fig. 2 is used to describe the level spacing distributions  $P(t)$ 's when  $p > p_c$ . In this case, the calculations of the functions  $P(t)$ 's are not very accurate because of the degeneracy of resonances. For a specific sample, it is impossible to estimate where the next level is due to the complex microstructure. However, for the disordered composites with a definite  $p$ , when the  $i$ th level is measured, the spacing between the  $i$ th and  $(i+1)$ th levels satisfies the ensemble averaged distribution  $P(t)$ , rather than the Poisson distribution  $P_p(t)$  or GOE case  $P_{WD}(t)$ . It is seen that the distributions  $P(t)$ 's lie between the profiles of the Poisson ensemble and GOE for  $p \in [0.1, 0.7]$ . As discussed in the introductory part, the critical  $P_T(t)$  approaches the  $P_{WD}(t)$  due to the strong interaction among the metallic bonds. When  $p$  is very small,  $P(t)$  is close to  $P_p(t)$  due to the weak interaction. At last, for an arbitrary  $p$ ,  $P(t)$  lies between the functions  $P_p(t)$  and  $P_T(t)$ . In this figure, it is also shown the crossover behavior of  $P(t)$ .

In Fig. 2, we find that the probability of small spacing is much less than the uncorrelated Poisson distribution. It means that some repulsion exists between neighboring levels. The repulsion in Gaussian ensembles comes from the symmetry of matrix elements. Here, the property of matrix elements is described by the Green's-matrix  $M$  of the GFF. So the repulsion of resonance levels is caused by the interaction of metallic bonds. The repulsion becomes stronger with decreasing  $|p - p_c|$ . For the GOE, we notice the importance of the repulsion law  $P(t) \propto t^\beta$  with  $\beta = 1$  for small spacing.<sup>1</sup> While for the composite materials with various  $p$ , when  $t \rightarrow 0.0$ ,  $P(t) > t^\beta$ . When  $t > 2.002$ , here 2.002 is the second intersection point of  $P_p(t)$  and  $P_{WD}(t)$ , the long tails of all functions approach the values of the Poisson ensemble.

### III. UNFOLDED LEVEL NUMBER VARIANCE

The above nearest neighbor level spacing distribution contains the information of short scales about the resonance spectrum. Long-range correlation is measured by the level number variance  $\Sigma^2(L)$ , given by<sup>1</sup>

$$\Sigma^2(L) = \langle C^2(L, \xi_s) \rangle - \langle C(L, \xi_s) \rangle^2, \quad (3)$$

where  $C(L, \xi_s)$  counts the number of levels in the interval  $[\xi_s, \xi_s + L]$  on the unfolded scale. The angular bracket denotes the average over the starting points  $\xi_s$ . By the unfolding,  $\langle C(L, \xi_s) \rangle$  should be equal to  $L$ . Thus, in the interval of length  $L$ , one expects to find the  $L \pm \sqrt{\Sigma^2(L)}$  levels on average. For the Poisson spectrum without correlation, one obtains  $\Sigma_p^2(L) = L$ , while for the GOE, the analytical result is

$$\Sigma_{WD}^2(L) = \frac{2}{\pi^2} (\ln(2\pi L) + \gamma + 1 - \frac{\pi^2}{8}), \quad (4)$$

where  $\gamma = 0.5772\dots$  is the Euler's constant. Fig. 3 shows the numerical results of level number variances  $\Sigma^2(L)$ 's for  $p \in [0.1, 0.7]$ . The same lines and symbols are used as those in Fig. 2, namely, the profiles of the Poisson ensemble and GOE are represented by the dashed and solid lines, and the critical level number variance  $\Sigma_T^2(L)$  is plotted by the solid line with the circles. It is obvious that the correlation among levels is greater than the Poisson case and less than the GOE case. We could not collect the data for  $p > 0.7$  due to the degeneracy of eigenvalues. When  $p = 0.1$  or  $p = 0.2$ , the level number variance  $\Sigma^2(L)$  is out of the boundary of the Poisson ensemble. The reason is that the data can not be fitted very well by the third or higher order polynomial in the unfolding procedure. For  $p \in [0.3, 0.7]$ ,  $\Sigma^2(L)$ 's lie between the profiles  $\Sigma_p^2(L)$  and  $\Sigma_T^2(L)$ . As shown in Fig. 3, the curves almost overlap for  $p = 0.4$  and  $p = 0.6$ , as well as for  $p = 0.3$  and  $p = 0.7$ . So at the percolation threshold, the crossover behavior of the level number variance is numerically obtained.

### IV. CROSSOVER AND FINITE SIZE SCALING AT PERCOLATION THRESHOLD

For a percolating network, level spacing distribution limited in the interval  $s \in [0.25, 0.75]$  has been investigated by Luck et. al..<sup>14</sup> Recent numerical calculations indicate that the

resonances within  $[0, 0.25]$  and  $[0.75, 1]$  are important because the high values of the inverse participation ratios (IPR) in those regions correspond to the strongly enhanced optical responses.<sup>16</sup> In order to study the criticality of level spacing distribution  $P(t)$  and level number variance  $\Sigma^2(L)$  in a two dimensional network, the duality of level spacing for binary model is discussed. We consider an infinite binary network with concentration  $p$ . The admittance of impurity bonds and matrix bonds is set to  $\epsilon_1$  and  $\epsilon_2$  respectively. We get the admittance ratio  $h = \epsilon_1/\epsilon_2$  and  $s = \frac{1}{1-h}$ . The resonance spectrum is given by the set  $\{s_1, s_2, \dots, s_n\}$ . Then the set  $\{t\}$  of level spacing can be written as  $\{t_1, t_2, \dots, t_{n-1}\}$  with  $t_{n-1} = s_n - s_{n-1}$ . For a large network,  $G$  is a typical configuration of the concentration  $p$ . Binary model is invariant under the simultaneous interchange  $p \leftrightarrow 1 - p$  and  $\epsilon_1 \leftrightarrow \epsilon_2$ . So  $G'$  is also a typical configuration of the concentration  $1 - p$  and we get the new admittance ratio  $h' = \frac{1}{h}$  and  $s' = 1 - s$ . The spectrum of resonance is replaced by the set  $\{s'_1, s'_2, \dots, s'_n\}$  with  $s'_1 = 1 - s_1, s'_2 = 1 - s_2$  and  $s'_n = 1 - s_n$ . The new level spacing set  $\{t'\}$  is just the original set  $\{t\}$ . So the duality of level spacing exists for the binary model and it is the self-dual at  $p = p_c = 0.5$ . The functions  $P(t)$  and  $\Sigma^2(L)$  are computed based on the same set  $\{t\}$  for  $p$  and  $1 - p$ .

In the calculations, we can not find the strict duality of level spacing. One reason is that the binary sample is not large enough. Another is that the degeneracy of resonances affects the accuracy of  $P(t)$  and  $\Sigma^2(L)$  when  $p > p_c$ . Numerical results indicate the crossover of level spacing distribution  $P(t)$  and level number variance  $\Sigma^2(L)$ , as shown in Fig. 4 and Fig. 5. To characterize this behavior, for each distribution  $P(t)$ , we compute the value  $\eta = \frac{\int_0^{t_0} [P(t) - P_{WD}(t)] dt}{\int_0^{t_0} [P_p(t) - P_{WD}(t)] dt}$  with  $t_0 = 0.4729$ , the first interaction point of  $P_p(t)$  and  $P_{WD}(t)$ .<sup>2,3</sup> In this way,  $\eta$  varies from  $1[P(t) = P_p(t)]$  to  $0[P(t) = P_{WD}(t)]$ . We note that  $\eta_T = 0.2162$  at the transition is close to the value  $\eta_A = 0.215$ , which corresponds to  $P_A(t)$  at the Anderson transition.<sup>18</sup> As observed in Fig. 4,  $\eta(p)$  is closer to the value 1 of the Poisson ensemble with increasing  $|p - p_c|$ . In Fig. 3, we have found the linear relation of  $\Sigma^2(L)$  with respect to  $L$  as  $\Sigma^2(L) = \chi * L$ , where  $\chi$  is called the spectral compressibility.<sup>6</sup> When the unfolded number  $L$  is larger, the value  $\chi$  is 1 for the Poisson ensemble, while for the GOE or Wigner-Dyson ensemble,  $\chi$  is approximately equal to 0. For various  $p$ , the slopes  $\chi$ 's are plotted in Fig. 5. At  $p_c$ ,  $\chi = 0.395$  is close to 0, rather than the value 1 of the Poisson ensemble. In Fig. 4 and Fig. 5, we observe the crossover behavior of  $P(t)$  and  $\Sigma^2(L)$ , as well as the duality of level spacing.

Finite size scaling of mean level spacing  $\delta$  and mean level number  $n$  are computed when the percolating sample is in size from  $16 \times 16$  to  $32 \times 32$ . For each case, more than 700,000 levels are calculated for the ensemble averaging. The results are shown in Fig. 6 and Fig. 7. Finite size scaling laws,  $\delta = 1.032L^{-1.952}$  and  $n = 0.911L^{1.970}$ , are obtained. Note that here the meaning of  $L$  is different from that in Fig. 3. The scaling exponents 1.952 and 1.970 are universal and closely related to the spatial dimension ( $D = 2$ ) of the network.

## V. CONCLUSIONS

We have investigated the fluctuation and correlation of geometric resonance level spacing in the random binary composites by RMT. The main conclusions include:

1. For a definite  $p$ , the unfolded level spacing  $P(t)$  and level number variance  $\Sigma^2(L)$  have the general features.
2. For an arbitrary  $p$ , the short-range spectral fluctuation  $P(t)$  and long-range spectral correlation  $\Sigma^2(L)$  lie between the profiles of the Poisson ensemble and critical ensemble.
3. The functions  $P_T(t)$  and  $\Sigma_T^2(L)$  at the transition approach the profiles of the GOE, rather than the profiles of the Poisson ensemble.
4. The crossover behavior and duality of  $P(t)$  and  $\Sigma^2(L)$  are found when  $p$  approaches  $p_c$ .
5. At  $p_c$ , finite size scaling laws,  $\delta = 1.032L^{-1.952}$  and  $n = 0.911L^{1.970}$ , are obtained.

Statistics of eigenvalues of the Green's-matrix  $M$  has been studied and the general statistical distributions have been obtained. Statistics of eigenvectors of  $M$ , which are closely related to the local electric fields, will be published elsewhere.

## REFERENCES

- [1] T. Guhr, A. Muller-Groeling, and H. A. Weidenmuller, Phys. Rep. **299**, 189 (1998).
- [2] Ph. Jacquod and D. L. Shepelyansky, Phys. Rev. Lett. **79**, 1837 (1997).
- [3] P. H. Song and D. L. Shepelyansky, Phys. Rev. B **61**, 15546 (2000).
- [4] IsaKh. Zharekeshev and B. Kramer, Phys. Rev. Lett. **79**, 717 (1997).
- [5] L. Schweitzer and I. K. Zharekeshev, J. Phys. Condens. Matter **7**, L377 (1995).
- [6] I. Varga and D. Braun, Phys. Rev. B **61**, R11859 (2000).
- [7] E. Cuevas, Phys. Rev. Lett. **83**, 140 (1999).
- [8] M. F. Law, Y. Gu and K. W. Yu, Phys. Rev. B **58**, 12536 (1998).
- [9] M. F. Law, Y. Gu and K. W. Yu, J. Phys. : Condens. Matter **10**, 9549 (1998).
- [10] M. I. Stockman, L. N. Pandey, L. S. Muratov, and T. F. George, Phys. Rev. Lett. **72**, 2486 (1994).
- [11] M. I. Stockman, L. N. Pandey, and T. F. George, Phys. Rev. B **53**, 2183 (1996).
- [12] V. M. Shalaev and A. K. Sarychev, Phys. Rev. B **57**, 13265 (1998).
- [13] J. P. Clerc, G. Giraud, J. M. Luck, and Th. Robin, J. Phys. A: Math. Gen. **29**, 4781 (1996).
- [14] Th. Jonckheere and J. M. Luck, J. Phys. A: Math. Gen. **31**, 3687 (1998).
- [15] Y. Gu, K. W. Yu and H. Sun, Phys. Rev. B **59**, 12847 (1999).
- [16] Y. Gu, PH.D Thesis, copyrighted by the Chinese University of Hong Kong (CUHK) (2001).
- [17] D. J. Bergman and D. Stroud, Solid State physics, **146**, 147 (1992).
- [18] B. I. Shklovskii, B. Shapiro, B. R. Sears, P. Lambrianides, and H. B. Shore, Phys. Rev. B **47**, 11487 (1993).

## FIGURES

FIG. 1. The typical cumulative spectral function  $C(s)$  of resonance levels. The small part of the measured spectrum is shown as the staircase function. The smooth part  $\xi(s)$  is the third order polynomial whose coefficients are found by a fit of the whole measured spectrum.

FIG. 2. Level spacing distribution  $P(t)$  of resonance spectrum on the unfolded scale. Here  $p$  is ranged at the interval  $[0.1, 0.7]$ . Dashed and solid lines show  $P(t)$ 's of the Poisson ensemble and GOE. The solid lines with filled or opaque symbols show the profiles of various  $p$ .

FIG. 3. Level number variance  $\Sigma^2(L)$  of resonance spectrum on the unfolded scale. Here  $p$  is ranged at the interval  $[0.2, 0.7]$ . Dashed and solid lines show  $\Sigma^2(L)$ 's of the Poisson ensemble and GOE. The solid lines with filled or opaque symbols show the profiles of various  $p$ .

FIG. 4. Dependence of  $\eta$  on the concentration  $p$ . The lines are guides to the eyes.

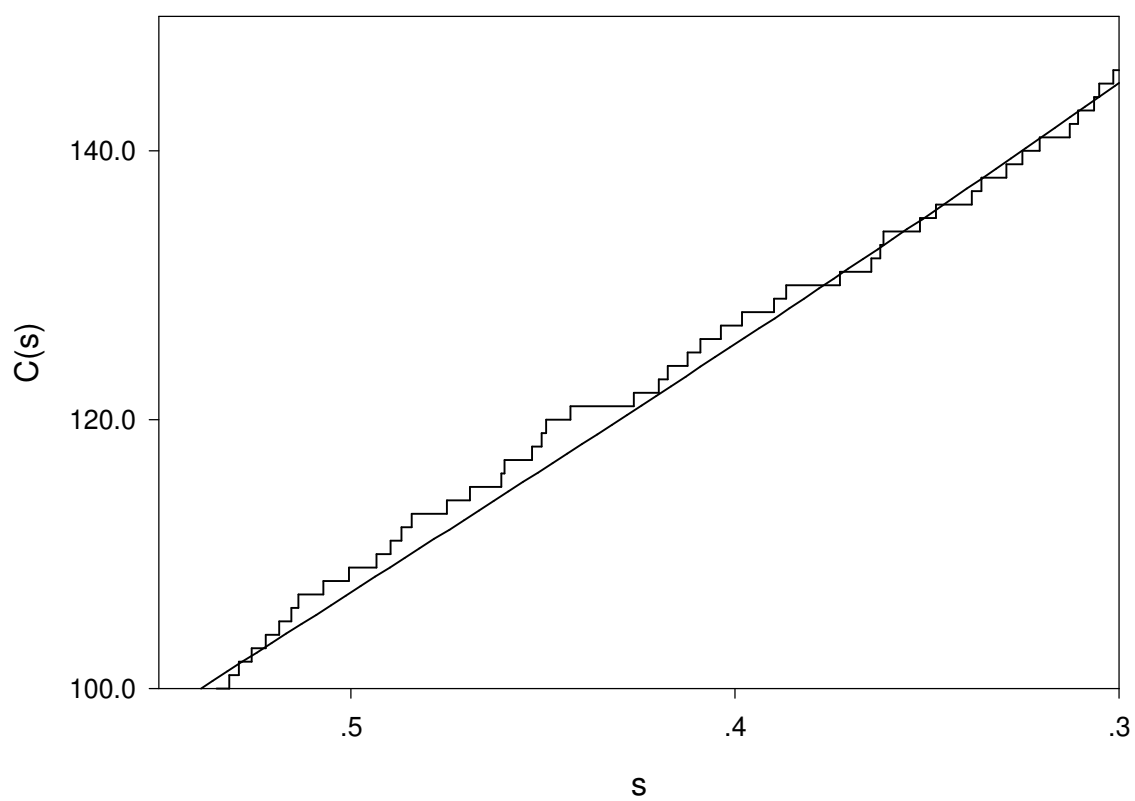
FIG. 5. Dependence of the spectral compressibility  $\chi$  on the concentration  $p$ . The lines are guides to the eyes.

FIG. 6. Finite size scaling of the mean level spacing  $\delta$  at  $p_c$ . The sample is in size from  $16 \times 16$  to  $32 \times 32$ .

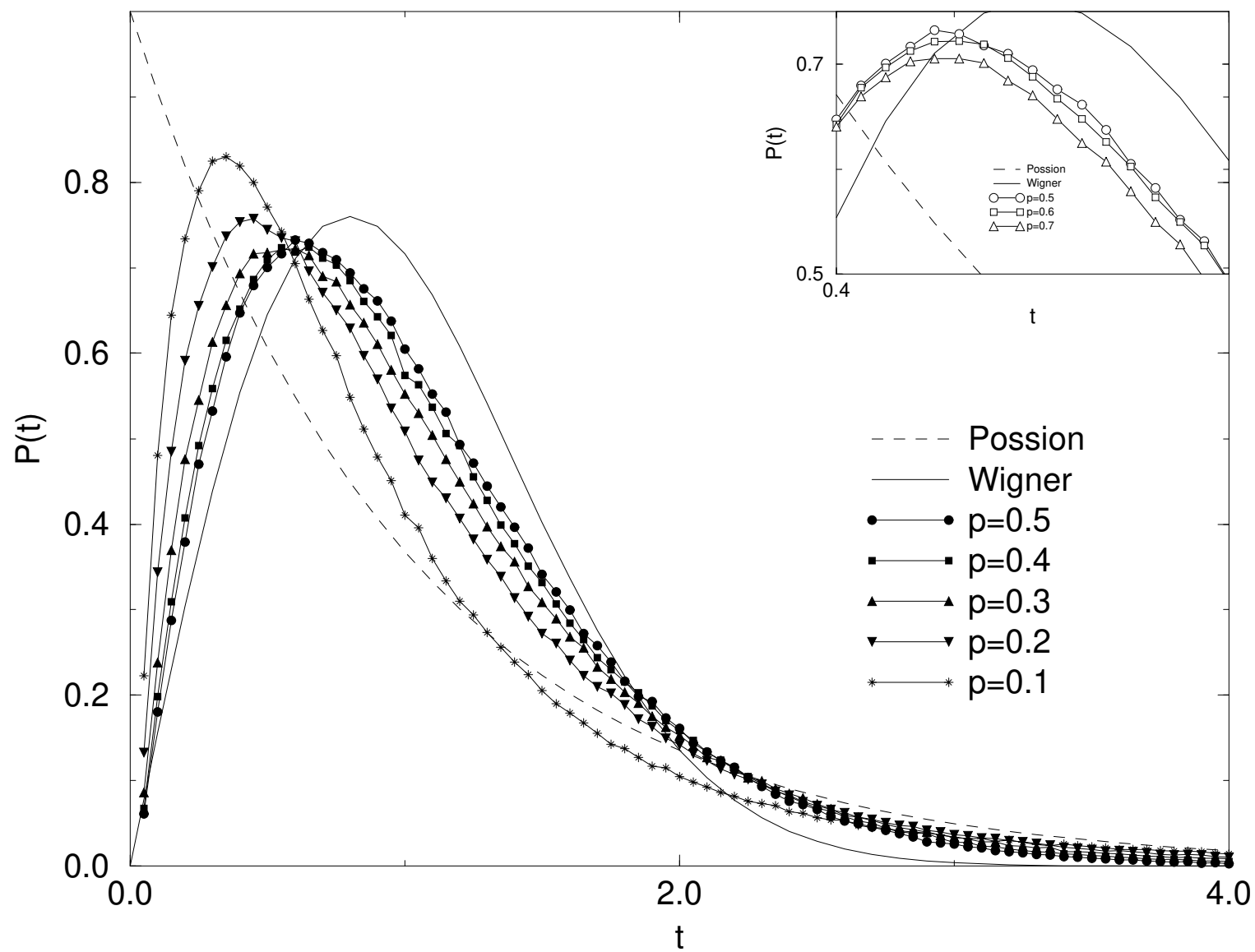
FIG. 7. Finite size scaling of the mean level number  $n$  at  $p_c$ . The sample is in size from  $16 \times 16$  to  $32 \times 32$ .

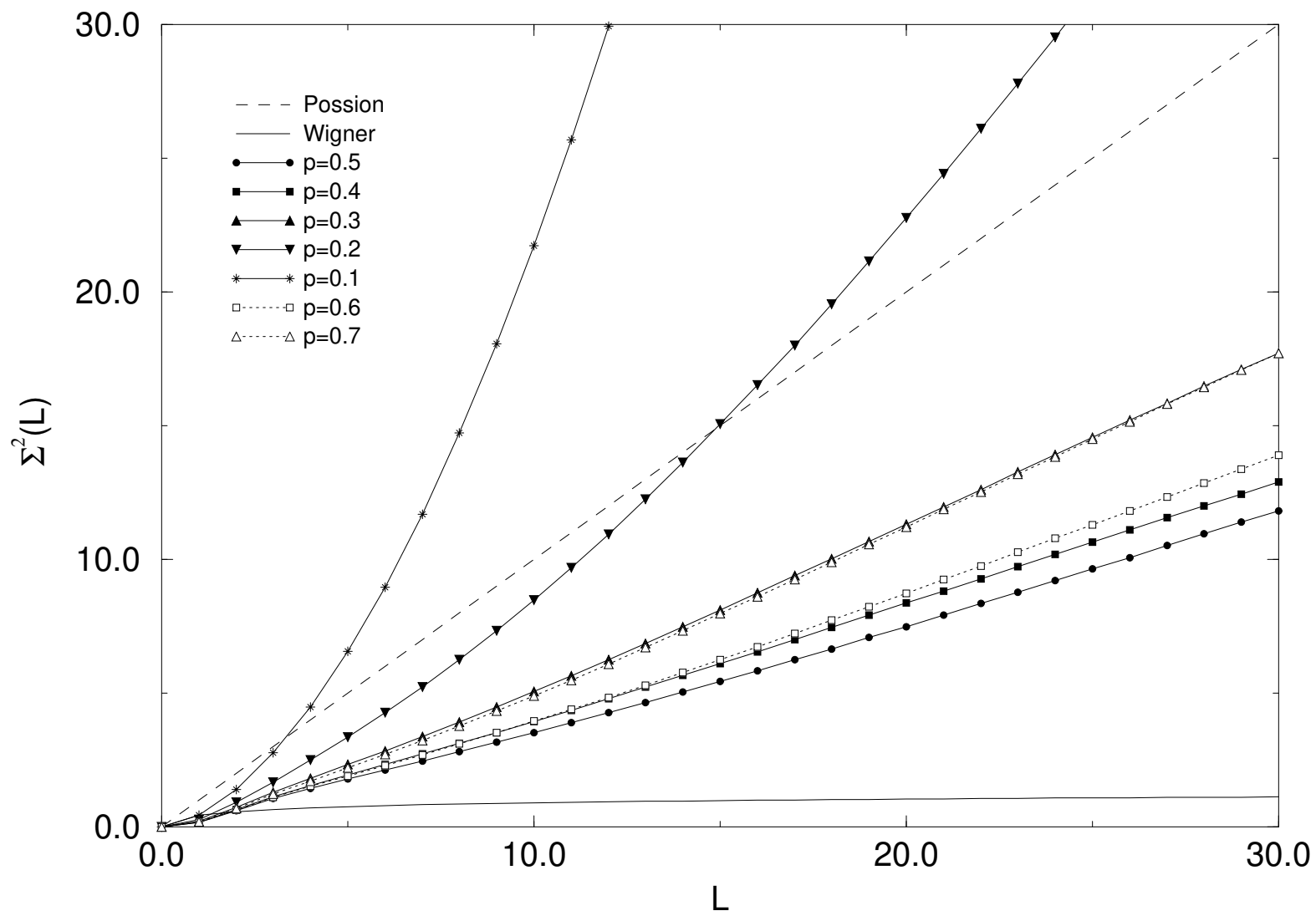


$L=16, p=0.5$ , cumulative spectral function  $C(s)$ .

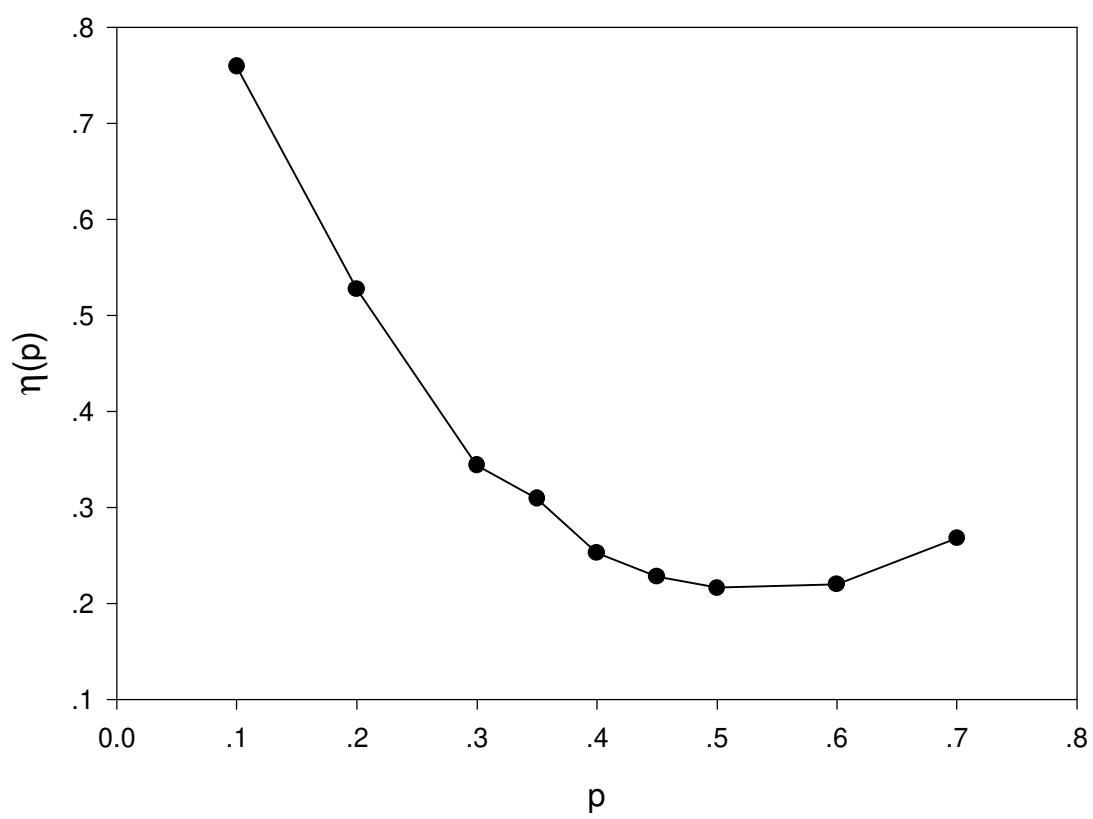






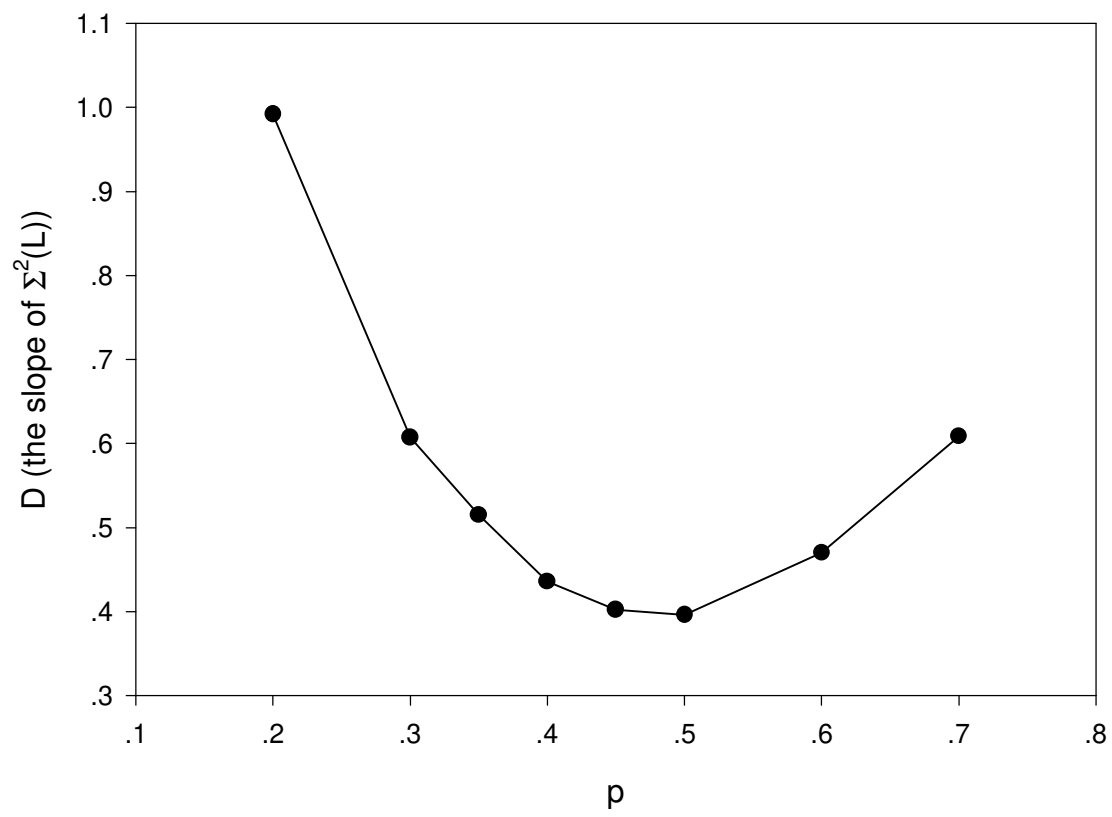


$\eta(p)$ ,  $p$  is ranged from 0.1 to 0.7.





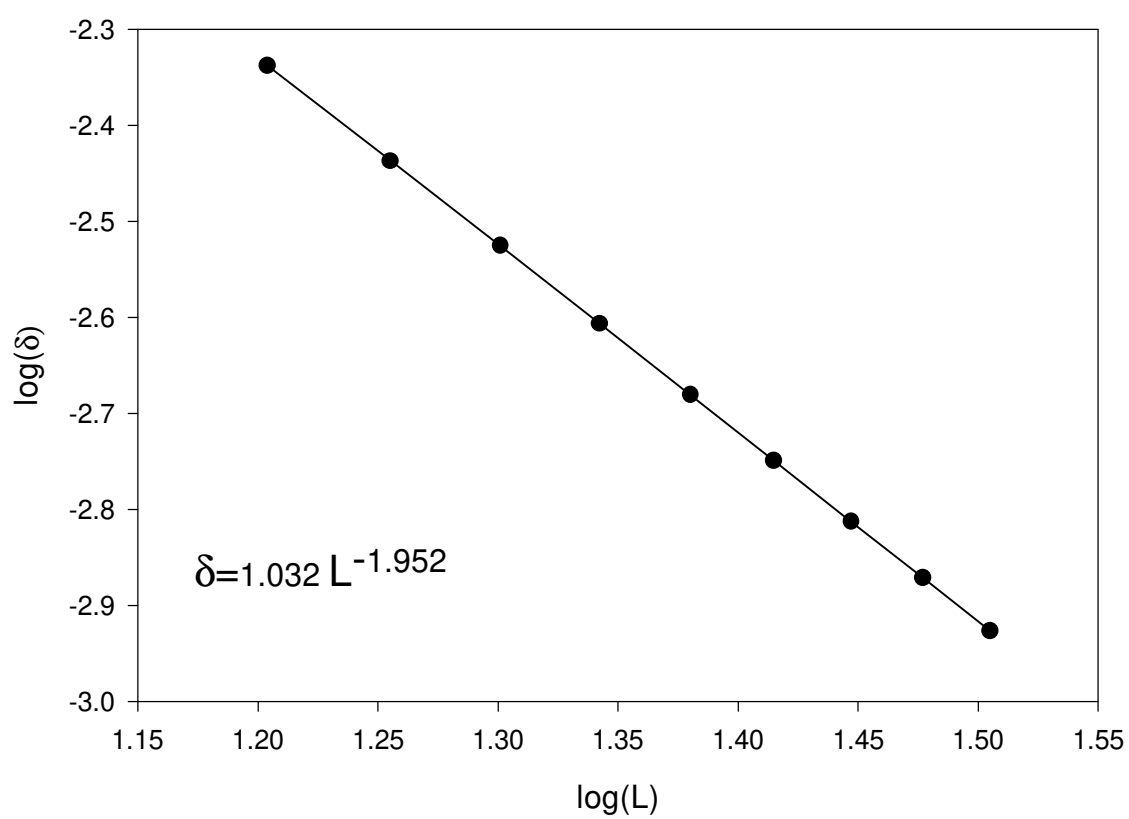
The slope D of  $\Sigma^2(L)$ , p is ranged from 0.1 to 0.7.







Finite size scaling of the mean level spacing  $\delta$ ,  
the sample size is changed from  $16 \times 16$  to  $32 \times 32$ .





Finite size scaling of the mean levels  $n$ ,  $p=p_c$ ,  
the sample size is changed from  $16*16$  to  $32*32$

